

Competition between in-plane and out-of-plane magnetization in exchange-coupled magnetic films

W. Kuch, Xingyu Gao,* and J. Kirschner

Max-Planck-Institut für Mikrostrukturphysik, Weinberg 2, D-06120 Halle, Germany

(Received 27 May 2001; published 8 January 2002)

The coupling between a Co layer with in-plane easy axis of magnetization and a Ni layer with out-of-plane easy axis across a nonmagnetic Cu spacer layer was studied by layer-resolved magnetic imaging. Photoelectron emission microscopy and magnetic circular dichroism in soft x-ray absorption as the magnetic contrast mechanism were used for the domain imaging. Crossed, wedge-shaped epitaxial Co and Cu layers of 3.5–5.7 atomic monolayers (ML) Co and 2.5–4.1 ML Cu were deposited onto 15 ML Ni/Cu(001). The competition between ferromagnetic interlayer coupling and the magnetic uniaxial anisotropies of the two magnetic layers leads to a noncollinear magnetization configuration at Cu thicknesses above 3.1 ML. The Ni magnetization is thereby in a canted state, whereas the Co magnetization is nearly in plane. The canting angle of the Ni magnetization can be tuned between the surface normal and $\approx 45^\circ$ by adjusting the Cu thickness. At a Cu thickness of approximately 3.1 ML a transition to a collinear in-plane configuration at lower Cu thicknesses is observed. This can be explained by a phenomenological expression including the fourth-order anisotropy of the Ni layer.

DOI: 10.1103/PhysRevB.65.064406

PACS number(s): 75.70.Ak, 75.70.Kw

I. INTRODUCTION

The coupling between two magnetic layers across a nonmagnetic spacer layer has attracted a lot of attention, motivated both by fundamental interest^{1–4} and by the prospect of applications in data storage, magnetic sensors, and magnetoelectronics.^{5–7} The magnetic interlayer interaction for metallic nonferromagnetic spacer layers is commonly described by a phenomenological expression for the coupling energy, $-J_1(\hat{m}_1 \cdot \hat{m}_2)$.^{1,2} Here \hat{m}_1 and \hat{m}_2 are the unit vectors of magnetization in the two magnetic layers. The interaction is characterized by the coupling constant J_1 , also termed the bilinear coupling constant, which includes electronic and magnetostatic contributions. Depending on the sign of J_1 either a parallel or antiparallel orientation of the two layer magnetizations is energetically preferred. Besides these collinear configurations also noncollinear coupling has been observed, especially for antiferromagnetic spacer layers.^{8–10} This noncollinear coupling is described by a higher-order term in $(\hat{m}_1 \cdot \hat{m}_2)$ favoring 90° alignment of the magnetization directions (“biquadratic coupling”). It appears as a consequence of roughness-induced spatial fluctuations in the sign of J_1 (Ref. 11) or in a model explicitly taking into account the antiferromagnetism of the spacer layer.¹² In contrast to that, a noncollinear magnetic configuration induced by different magnetic anisotropies in the individual magnetic layers was recently proposed by Taga *et al.*¹³ Calculations for [Fe/V/Co/V] multilayers yielded for a certain thickness combination a magnetic configuration in which the Co layers are magnetized perpendicular to the film plane (“out of plane”), whereas the Fe magnetization is in the film plane (“in plane”).¹³ This is a direct consequence of orthogonal easy axis directions in the Co and Fe layers. In the absence of interlayer coupling the magnetic easy axes are defined by separate minimization of the anisotropy energy in each layer. Considering coupling between layers of different easy axes, the magnetization directions are determined by the competition between the anisotropy energy and the coupling energy.

In the case of a strong coupling, \hat{m}_1 and \hat{m}_2 are forced to be collinear, whereas for weak coupling the individual magnetization directions will be along the respective easy axes. Reorientation transitions between these two situations will occur for intermediate coupling as a function of the coupling strength. In the course of these reorientation transitions, depending on the angular shape of the anisotropy energy contours, also noncollinear configurations with obliquely canted magnetization directions can be expected even at zero field.

An example of epitaxial films that exhibit different magnetic easy axes for growth on the same substrate are ultrathin Ni and Co films on Cu(001): Whereas Co films are always magnetized in the film plane,^{14,15} Ni films show a perpendicular magnetization in an extended thickness range.^{16–18} The possibility of a canted magnetization in Co/Cu/Ni trilayers had been discussed by Lauhoff *et al.* based on the observation of reduced remanence of both films in neutron diffraction experiments. However, a multidomain state of the sample, leading possibly to the same observations, could not be ruled out.¹⁹ A reduced remanence of the Ni layer in the direction of the Co layer magnetization has been reported recently by Scherz *et al.* in Ni/Cu/Co trilayers on Cu(001) in a thickness range where both magnetic layers exhibit in-plane easy axes.²⁰ It was discussed as a noncollinear configuration of in-plane magnetizations due to the interplay of antiparallel coupling ($J_1 < 0$) and the temperature-dependent coercivity of the Ni layer.²⁰ However, a dominant contribution of biquadratic coupling or a multidomain state could not be ruled out.

We present in this paper a layer-resolved photoelectron emission microscopy (PEEM) study of the magnetic domain patterns of Co/Cu/Ni trilayers, epitaxially grown on Cu(001). From element-selective domain patterns of the as-grown films we can directly extract the local magnetization vector. The element selectivity is provided by x-ray magnetic circular dichroism (XMCD), which is used as a magnetic contrast mechanism for the PEEM domain images. The x-ray absorption cross section at elemental absorption maxima thereby depends on the relative orientation of the helicity vector of

the circularly polarized incoming x-rays and the magnetization direction in the sample.²¹ This allows one to image the domain configuration in each magnetic layer separately. Definite conclusions about canted and noncollinear magnetization configurations can be drawn, independent of domain formation. We show that for appropriate layer thicknesses a reorientation transition in the Ni layer between a noncollinear out-of-plane configuration and a collinear in-plane configuration occurs, during which the Ni assumes a canted magnetization. The canting angle can be tuned in a large range by varying the interlayer coupling strength, i.e., by varying the Cu spacer layer thickness.

II. EXPERIMENT

The measurements were performed at the helical undulator beamline UE56-2 of BESSY II in Berlin. Circularly polarized light emitted in the fifth harmonic of the undulator with a degree of polarization of about 80% was used, incident to the sample under an angle of 60° from the surface normal.

In PEEM the local secondary electron yield at the sample surface is used to create a magnified image of the sample, which is proportional to the local absorption and thus to the projection of the local magnetization direction onto the light incidence direction.²² A vectorial characterization of the magnetization direction within magnetic domains is achieved by rotating the sample about the surface normal and acquiring images of the same spot on the sample for different light incidence azimuths.

The setup of the electrostatic photoelectron emission microscope (Focus IS-PEEM) is identical to that described in previous publications.²³ In short, it consists of an electrostatic straight optical axis microscope with an integral sample stage and a variable-contrast aperture. The magnified image is intensified by a two-stage microchannel plate and converted into visible light by means of a scintillator crystal. The image is then computer recorded with 12-bit resolution by a Peltier-cooled camera (PCO SensiCam), which was operated with 2×2 binning of pixels. Parameters were set to result in a lateral resolution of 0.4 μm and a field of view of 60 μm. Images are presented in the form of grayscale-coded absorption asymmetry for opposite light helicity at the maxima of the Ni and Co L_3 edges, respectively. The acquisition times for the images presented here were 6 min for each helicity. For the quantitative analysis pre-edge images acquired at 5 eV lower photon energy were subtracted prior to evaluation of the XMCD asymmetry.

Co/Cu/Ni films on Cu(001) were grown and imaged at room temperature in an ultrahigh-vacuum chamber (base pressure 1×10^{-8} Pa in the sample preparation chamber and 2×10^{-8} Pa in the PEEM chamber) equipped with standard facilities for sample preparation and surface characterization. Nickel, copper, and cobalt films were evaporated by electron bombardment from high-purity material. Deposition rates were around 0.5 atomic monolayers (ML) per minute. Film thicknesses were derived from medium-energy electron diffraction oscillations during growth and Auger electron spectroscopy. The accuracy of the cited thicknesses is estimated

as 10% for Ni and Co and 20% for Cu. Cu and Co were prepared as crossed wedges by positioning 2×0.5 mm² slit apertures in front of the sample and rocking the sample and mask assembly about the long axis of the aperture during film deposition, as described in Ref. 24.

III. RESULTS

Figure 1 shows domain images obtained at the Co L_3 edge (left) and the Ni L_3 edge (right) of a Co/Cu crossed double wedge on 15 ML Ni/Cu(001). The Co thickness varies in the range of Fig. 1 from 3.5 to 5.7 ML from bottom to top, as indicated at the left axis, and the Cu thickness from 2.5 to 4.1 ML from left to right, as indicated at the bottom axis. Different colors correspond to different projections of the local magnetization direction onto the direction of incoming light, which is 30° from above the surface in the direction indicated in the bottom right corner of the left image. The legend in the right upper corner of the figure indicates the colors for positive and negative asymmetry, corresponding to parallel and antiparallel alignments of the local magnetization direction and light incidence. Only four different types of domains are recognized in the Co image. Most of the area is covered by relatively big stripelike domains showing a dark-blue and yellow contrast. At the top of the image also smaller domains with two intermediate colors, light blue and green, are present. Analysis of these four contrast levels reveals that the Co magnetization direction is in the film plane over the whole image, oriented along the four $\langle 110 \rangle$ crystal axes, as indicated by arrows. The average domain size in the upper part of the image is smaller than in the lower part. Such locally varying domain size differences in Co/Cu(001) ultrathin films have been already observed previously.²⁵

Inspection of the Ni image of Fig. 1 shows that the leftmost third of the image exhibits an identical domain pattern as the Co image. The three different color levels that are mainly observed in this part of the image exhibit the same relative size for Ni and Co. The Ni magnetization is here consequently also in plane, aligned with the Co magnetization direction, as shown by arrows.

A slightly tilted meandering vertical line, starting at about 3.1 ML Cu thickness in the bottom of the image, as indicated by the horizontal bar, and reaching the top at about 3.3 ML Cu thickness, separates this aligned in-plane region from the region at the right-hand side, which exhibits a gradual change of contrast. This change of contrast is seen best in the big stripelike domains in the lower half of the images. A gradual change from green to light blue is seen when following the stripes corresponding to blue domains in the Co image from right to left. This is explained by a canted magnetization in the Ni film, where the canting angle is gradually changing as a function of Cu thickness. Two sketches at the right-hand side of Fig. 1 illustrate the situation. The green Ni contrast in the blue Co domains is generated by a perpendicular Ni magnetization component pointing out of the surface plane (upper sketch). This leads to an antiparallel component of the magnetization direction with respect to the light propagation vector. The light blue contrast in the yellow

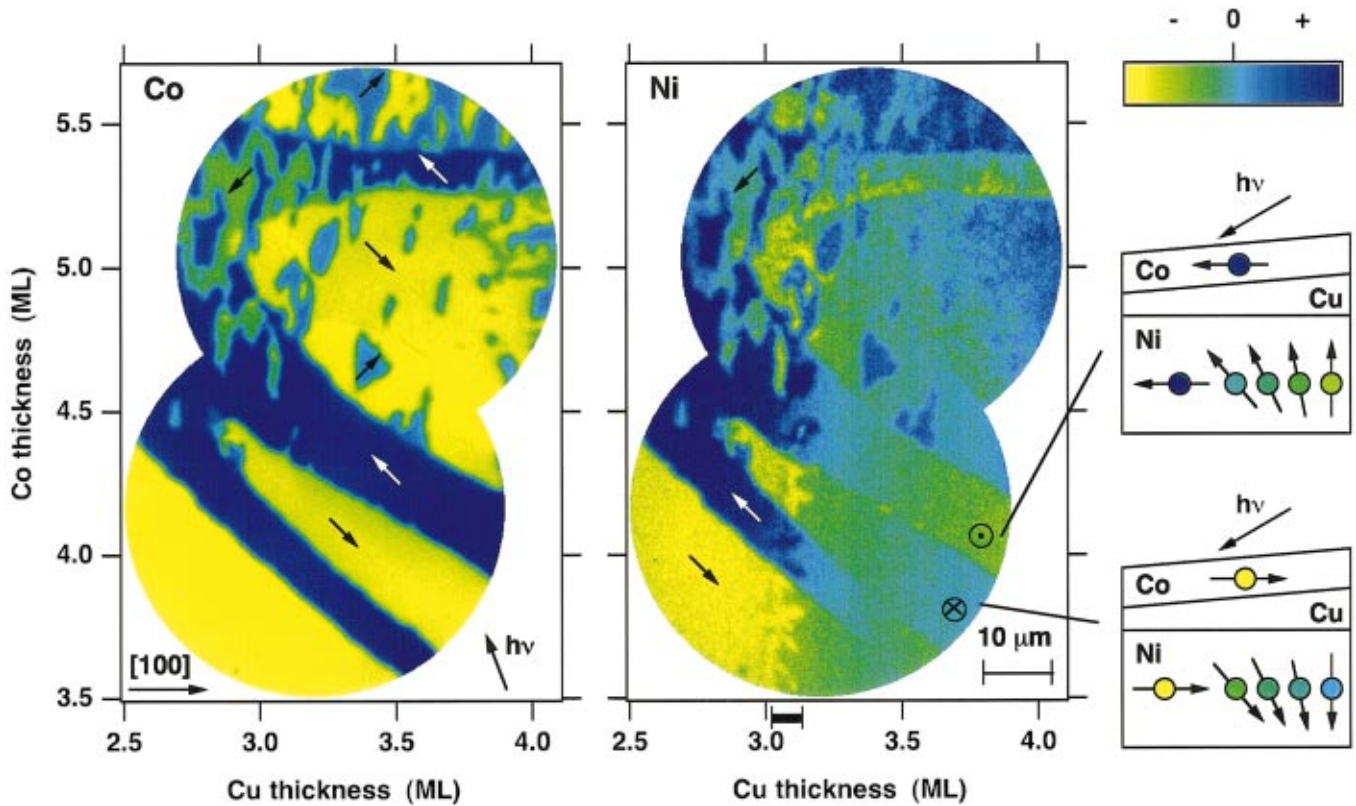


FIG. 1. (Color) Layer-resolved domain images of Co (left) and Ni (right) of 3.5–5.7 ML Co/2.5–4.1 ML Cu/15 ML Ni/Cu(001). Co and Cu thicknesses are indicated at the left and bottom axes, respectively. Whereas the Co layer in the entire image is magnetized in plane along the four $\langle 110 \rangle$ directions as indicated by arrows, the Ni layer shows a gradually changing canted magnetization direction at Cu thicknesses above 3 ML, as illustrated by the sketches on the right-hand side.

Co domains is explained equivalently by a perpendicular magnetization component pointing into the surface plane (lower sketch). For decreasing Cu thickness the Ni magnetization is increasingly canted into the local Co in-plane direction, until it suddenly switches into the aligned in-plane orientation. The color in the Ni image between these two domains thus reverses as a function of Cu thickness. At the zero crossing of the asymmetry—that is, where both domains show identical colors—the magnetization direction is perpendicular to the light incidence. Summarizing the observations from Fig. 1, we have a collinear region at small Cu thicknesses, in which both the Ni and Co moments are aligned and in the film plane, and a noncollinear region at higher Cu thicknesses, in which Ni shows a canted magnetization direction, whereas Co is magnetized in plane. The above-mentioned meandering line at 3.1–3.3 ML Cu thickness separates these two regions.

If we distinguish the Ni domains at the right-hand side of the image only with respect to their perpendicular magnetization component, three stripelike domains are observed in which the out-of-plane component of the Ni magnetization points up, separating bigger areas in which the Ni out-of-plane component points down. All the smaller domains that are mainly present in the upper part of the image differ only in their in-plane component, which means by the azimuthal orientation of the canting direction, induced by the corresponding in-plane Co domains. A clear correlation between

the Ni out-of-plane domains and the Co in-plane domains can be seen when comparing the Ni and Co domain patterns. In the part of the sample imaged here predominantly dark blue, i.e., $[\bar{1}10]$ -oriented, Co domains are found on top of “up” domains of Ni and yellow ($[1\bar{1}0]$ -oriented) domains on top of Ni “down” domains. The exact mechanism leading to this domain correlation is at present not fully clear and is the subject of further investigation.

A quantitative analysis of the Ni canting angle is shown in Fig. 2. It shows the Ni magnetization angle Θ in the plane spanned by the surface normal and the local Co in-plane magnetization direction as a function of Cu spacer layer thickness. Pure out-of-plane magnetization is defined as 90° , whereas 0° means in-plane magnetization aligned with the Co magnetization. The data points of Fig. 2 were obtained by a discriminating pixel-by-pixel analysis considering only regions of dark blue and yellow domains in Co, respectively, and averaging pixels belonging to the same Cu thickness. The analysis shows that at the right-hand side of Fig. 1, at around 4 ML Cu thickness, the Ni magnetization is canted by more than 20° away from the out-of-plane direction. For decreasing Cu thickness the Ni magnetization is tilted further into the direction of Co magnetization, until at around 3.2 ML Cu thickness and $\Theta \approx 45^\circ$ it turns completely into the in-plane direction (0°). In Fig. 2 this switching into the in-plane direction is not recognized as the sudden event that it is

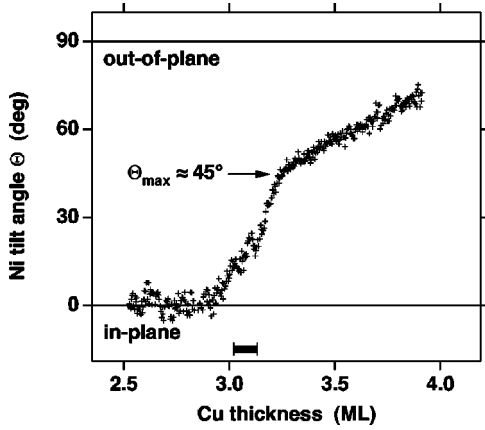


FIG. 2. Quantitative analysis of the Ni canting angle as a function of Cu spacer layer thickness, averaged along the vertical direction of Fig. 1. 90° corresponds to the out-of-plane direction, 0° to the in-plane direction.

in Fig. 1. Two reasons account for that: First, the line in Fig. 1 at which the Ni magnetization switches from the canted into the aligned orientation is not a straight line, but shows meandering of the order of about 0.1 ML Cu thickness variation, as indicated by the horizontal bars at the bottom of Figs. 1 and 2. Second, there is also a small dependence of the position of this line on Co thickness, which is neglected when plotting the canting angle as a function of Cu thickness. Both together lead to an artificial smearing out of the transition of about 0.3 ML Cu thickness in Fig. 2.

IV. DISCUSSION

The canting of the Ni magnetization into the direction of Co magnetization can be understood from the competition of the magnetic interlayer coupling between Ni and Co layers and the magnetic anisotropy of each of the two layers. We assume that in the Cu thickness range of Fig. 1 the coupling between Ni and Co favors ferromagnetic alignment and decreases with increasing Cu thickness. Furthermore, for the Ni and Co thicknesses investigated here, we can safely assume that the magnetic anisotropy is out of plane for the Ni layer and in plane for the Co layer. Whereas the perpendicular anisotropy of the Ni layer tends to orient the Ni magnetization out of plane, the ferromagnetic interlayer coupling tries to align it parallel with the Co moment, thus leading to a canted configuration. Since the Co in-plane anisotropy is much stronger than the Ni out-of-plane anisotropy, this will have only little effect on the Co magnetization direction.

In the limit of small canting of the Co magnetization, the interlayer coupling acts on the Ni layer in the same way as an external magnetic field, provided that the layer thickness is small compared to the exchange length, as is the case here. Spin-reorientation transitions in the presence of an external field have been theoretically investigated by Millev *et al.*³⁰ It has been outlined by these authors that transitions between canted and conforming phases (the latter has to be identified with our collinear phase) occur only for opposite sign of second-order anisotropy constant K_2 and fourth-order anisotropy constant k_4 , where the anisotropy energy is expanded

into a power series of even powers of $\cos(\Theta)$, keeping only the first two terms, i.e., $K_2\cos^2(\Theta) + k_4\cos^4(\Theta)$. Here Θ is the angle between the magnetization and the film plane. The uppercase letter of K_2 indicates that the *effective* uniaxial anisotropy is meant, which includes the magnetostatic demagnetizing energy $-\frac{1}{2}\mu_0M^2$, i.e., $K_2 = k_2 - \frac{1}{2}\mu_0M^2$. Applying a field along the hard axis leads in this case to a gradual canting of the magnetization away from the easy axis into the field direction, followed by an abrupt transition into the hard axis for higher fields.³⁰ Qualitatively the same behavior is observed in the Co/Cu/Ni trilayers.

To describe the more general case of two coupled magnetic layers we have to consider the anisotropy energy of both layers. The free energy F of the Co/Cu/Ni trilayer can be phenomenologically written as

$$F(\Theta_{Co}, \Theta_{Ni}) = K_{2,Co}\cos^2(\Theta_{Co}) + K_{2,Ni}\cos^2(\Theta_{Ni}) + k_{4,Ni}\cos^4(\Theta_{Ni}) - J_1\cos(\Theta_{Co} - \Theta_{Ni}). \quad (1)$$

The first term on the right-hand side describes the anisotropy of the Co layer, the next two terms the anisotropy of the Ni layer, and the last term the interlayer exchange coupling between Co and Ni layers. Since the fourfold in-plane anisotropy of 15 ML Ni/Cu(001) was reported to favor the $\langle 110 \rangle$ directions,¹⁸ which coincides with the easy axis of magnetization in Co/Cu(001),^{14,15} only magnetization directions within the $(1\bar{1}0)$ plane—i.e., the plane containing the $[001]$ surface normal and the $[110]$ in-plane direction—are considered here. For Co we have included only the first term of the expansion in $\cos^2(\Theta)$, which is sufficient since the Co magnetization deviates only very little from the in-plane direction. In the expression for the Ni anisotropy also the fourth power in $\cos(\Theta_{Ni})$ has been included in order to model the sudden switching of the Ni layer into the aligned direction. Similar to the case of spin reorientation transitions in an external field, a fourth-order contribution of opposite sign compared to K_2 is necessary to describe the sharp transition between noncollinear and collinear magnetization. Since $K_{2,Ni}$ is positive (out-of-plane easy axis), a negative fourth-order contribution is needed.

For the numerical modeling we have chosen literature values for $K_{2,Co}$ and $K_{2,Ni}$. From Ref. 15 we get $K_{2,Co} = -760 \mu\text{eV/surface atom}$ for 4 ML Co/Cu(001) and from Ref. 18 $K_{2,Ni} = +107 \mu\text{eV/surface atom}$ for 15 ML Ni/Cu(001), where we have already included magnetostatic energies of $\frac{1}{2}\mu_0M_{Co}^2 = 87.0 \mu\text{eV/atom}$ and $\frac{1}{2}\mu_0M_{Ni}^2 = 11.6 \mu\text{eV/atom}$. The maximum canting angle Θ_{max} depends very sensitively on the ratio between $k_{4,Ni}$ and $K_{2,Ni}$. From the experimentally observed value $\Theta_{max} \approx 45^\circ$, $k_{4,Ni}/K_{2,Ni} = -0.29$ and, hence, $k_{4,Ni} = -31 \mu\text{eV/surface atom}$ is determined. The out-of-plane components M_\perp/M for the Ni and Co layers as a function of the bilinear coupling constant J_1 are shown in Fig. 3 as solid and dashed lines, respectively. They were obtained by tracing the local minimum of Eq. (1) in Θ_{Ni} and Θ_{Co} , starting from $J_1 = 0$, where Ni is fully out of plane. Note that hysteresis and metastability can occur in the minimization of Eq. (1) due to the presence of two local

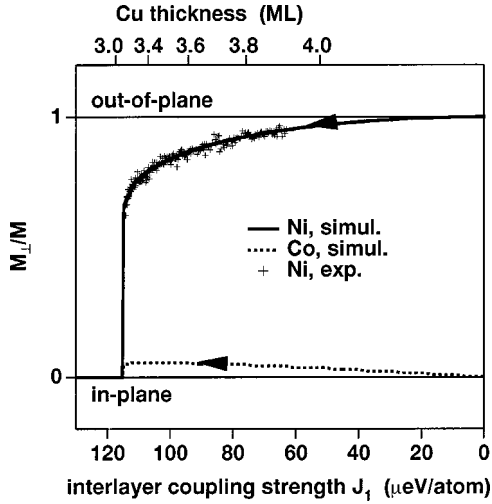


FIG. 3. Result of modeling the magnetization direction tilt in Co/Cu/Ni by Eq. (1). Shown are the out-of-plane components of the magnetization of the Ni layer (solid line) and of the Co layer (dotted line) for increasing bilinear interlayer coupling constant J_1 . 1 corresponds to the out-of-plane direction, 0 to the in-plane direction. Parameters used were $K_{2,Co} = -760 \mu\text{eV}/\text{surface atom}$, $K_{2,Ni} = +107 \mu\text{eV}/\text{surface atom}$, and $k_{4,Ni} = -31 \mu\text{eV}/\text{surface atom}$. The markers represent experimental data, where increasing coupling strength has been identified with decreasing Cu spacer layer thickness, as indicated at the upper axis.

minima in $F(\Theta_{Ni})$. Tracing the local energy minimum from $M_{NiL}/M_{Ni} = 1$ takes into account the experimental situation, where the Ni film is first magnetized out of plane before the Co overlayer is deposited. In the reverse case, when the Ni layer is first magnetized in plane, the respective jump to the canted magnetization upon decreasing coupling strength would occur at a smaller J_1 . For the above anisotropy values the transition from canted to in plane magnetization is calculated to occur at $116 \mu\text{eV}/\text{atom}$, whereas the jump from in plane to canted would be at $92 \mu\text{eV}/\text{atom}$.

One can see that the experimental results concerning the gradual canting of the Ni magnetization and the sudden jump to in-plane orientation are reproduced by that simple model if we identify the decreasing Cu spacer layer thickness with increasing coupling strength J_1 . From comparison of Figs. 1 and 3 it is possible to extract the coupling strength as a function of Cu film thickness, keeping in mind that the absolute values of J_1 depend on the assumption of the above literature values of K_2 . This is shown in Fig. 4. The markers represent the experimental data points; the solid line is a parabolic fit to the data. The magnitude of the coupling strength J_1 corresponding to the range of Cu thicknesses imaged in Fig. 1 is in reasonable agreement with what is usually observed.¹ We do, however, not find negative values for J_1 in that thickness range. In a recent paper about Curie temperature shifts in exchange-coupled Co/Cu/Ni/Cu(001) samples Ney *et al.* also observe a decreasing coupling strength with increasing Cu thickness above 3 ML.²⁶ A small negative maximum of J_1 between 3.5 and 4.0 ML Cu thickness, however, is present in Ref. 26 and attributed to the short-period oscillation of J_1 . This is not seen in the present

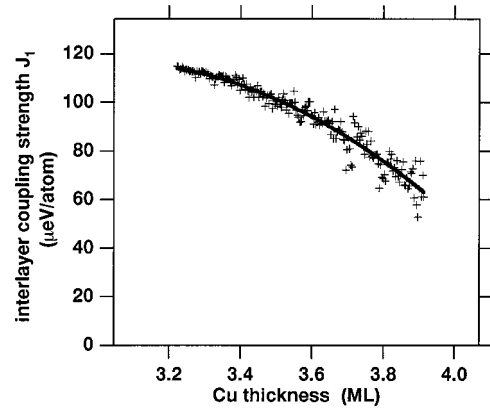


FIG. 4. Interlayer coupling strength J_1 as a function of Cu film thickness. Markers: experimental data points from Fig. 2, mapped onto the model curve from Fig. 3. Line: parabolic fit to the data.

data. We attribute that to the different Ni layer thickness, 15 ML in contrast to 3.0–4.8 ML in Ref. 26, which leads to a significantly higher roughness of the films.²⁷ A higher interface roughness in turn leads to a stronger damping of the short period oscillation²⁸ and to a stronger superimposed contribution from ferromagnetic magnetostatic coupling (so-called “orange-peel” coupling²⁹), which are likely responsible for the absence of antiparallel coupling in our samples.

Using the fit to the data from Fig. 4, the experimental data points for the Ni out-of-plane magnetization component can be plotted as a function of coupling strength. This is done in Fig. 3, where the markers illustrate the range probed in the present experiment. The corresponding Cu spacer layer thicknesses are given at the upper axis.

From the above model it follows that also the Co magnetization is canted away from the in-plane direction by up to 3° . This is, however, too small to be recognized in the PEEM experiment. As discussed above, in that case the action of the Co layer on the Ni layer, mediated by the interlayer coupling, is similar to that of an external field. For $\Theta_{Co} = 0$, Eq. (1) reduces to the expression for the free energy of a single Ni layer in an external in-plane magnetic field \mathbf{H} , where the coupling term $-J_1 \cos(\Theta_{Ni})$ can be identified with the Zeeman energy $-\mathbf{H} \cdot \mathbf{M}_{Ni} = -HM_{Ni} \cos(\Theta_{Ni})$. The field H which would be necessary for canting the Ni layer to the maximum angle of 45° is calculated to be 2065 Oe, using the above Ni anisotropy parameters.

The coupling-induced spin-reorientation transition of the Ni layer in the Co/Cu/Ni trilayers is qualitatively different from thickness or temperature induced spin-reorientation transitions in single magnetic ultrathin films. In the latter a canted magnetization occurs only in the presence of a positive fourth-order anisotropy term in the phenomenological expansion of the anisotropy energy,^{18,31–34} which leads to a continuous, second-order-like transition. Canting is not observed during a first-order-like transition. The spin reorientation-transition mediated by the interlayer coupling, on the other hand, can show a canted magnetization for both signs of the fourth-order term. The fourth-order term again describes the type of the transition, continuous or discontinuous. In the present example of Co/Cu/Ni trilayers we observe

the discontinuous type, characterized by the absence of canting angles below 45° from the plane of the film.

The magnetocrystalline anisotropy of bulk Ni favors the $\langle 111 \rangle$ directions as easy axes and thus would contribute with a positive sign to $k_{4,Ni}$ in Eq. (1). From the room-temperature anisotropy constant of bulk Ni,³⁵ however, a possible contribution from bulk anisotropy is calculated to be only $0.3 \mu\text{eV}/\text{atom}$, or $4.5 \mu\text{eV}/\text{surface atom}$ for 15 ML Ni, which is clearly weaker than the negative fourth-order anisotropy observed here. Extrapolation of the ferromagnetic resonance data of Farle *et al.* to 15 ML also yields a fourth-order anisotropy with (in our nomenclature) a positive sign of $+21 \mu\text{eV}/\text{surface atom}$.¹⁸ However, these data were recorded from Ni films of 6.7–8.0 ML thickness on Cu(001), which is exactly the thickness at which the authors observe the reorientation of the easy axis of magnetization of Ni/Cu(001) from in plane to out of plane. A fourth-order anisotropy with a positive sign at a thickness close to the spin-reorientation transition can be caused by thickness fluctuations, which lead to spatial fluctuations of the sign of the second-order anisotropy.³⁶ This mechanism is similar to the one used to explain the biquadratic interlayer coupling.¹¹ At 15 ML Ni thickness, which is clearly above the spin-reorientation transition thickness of single Ni films on Cu(001), this positive contribution to k_4 would be much reduced, so that an intrinsic negative contribution could show up. The different environment and different interfaces in Ni/Cu(001) and Co/Cu/Ni/Cu(001) could also account for the different sign.

We have to recall at that point that the expansion of anisotropy energy into a power series of $\cos(\Theta)$ is just a phenomenological description of the intrinsic angular dependence of the anisotropy energy. This energy is determined by changes in the electronic structure corresponding to the symmetry character of the respective magnetization direction.³⁷ Since small changes of the total band energy are sufficient to account for the observed size of anisotropies, geometrical details like strain and interface roughness as well as hybridization with adjacent layers will have a sizable influence. The occurrence of continuous or discontinuous spin-reorientation transitions depends in a very sensitive way on the system parameters.³⁸ The value of $k_{4,Ni}$ directly influences the maximum canting angle of the Ni magnetization and, thus, the Cu thickness at which the jump to the collinear configuration occurs. The meandering shape of the transition line between the noncollinear canting phase and the collinear in-plane phase seen in Fig. 1 indicates indeed a sensitive dependence of $k_{4,Ni}$ on local properties in the film. Local fluctuations in the Cu transition thickness of 0.1 ML correspond to changes in $k_{4,Ni}$ of $1.5 \mu\text{eV}/\text{surface atom}$.

A possible biquadratic contribution to the interlayer coupling has been neglected in our model. In the limit of small canting of the Co magnetization the effect of a biquadratic coupling, which is represented by an energy term $-J_2 \cos^2(\Theta_{Co} - \Theta_{Ni}) \rightarrow -J_2 \cos^2(\Theta_{Ni})$, would be indistinguishable from a modification of the value of $K_{2,Ni}$.

The weak dependence on Co thickness of the transition line between the canted and aligned phases seen in Fig. 1 is also reproduced in the model of Eq. (1). The coupling

strength at which the switching to the aligned in-plane magnetization occurs depends on $K_{2,Co}$ and, thus, on Co thickness. If the Co layer has a stronger in-plane anisotropy (more negative $K_{2,Co}$), the Co magnetization will be canted less away from the 0° in plane direction, which leads to a higher torque on the Ni magnetization, which in turn is equivalent to a stronger coupling. The transition to in plane will thus happen at smaller interlayer coupling strength for higher Co anisotropy or, in other words, at a higher Cu thickness for higher Co thicknesses. Since the Co canting angle is small, the variation of the Cu thickness of the reorientation transition will also be small. This is exactly what is observed in Fig. 1. This dependence on Co thickness makes it very implausible that a sudden drastic increase in coupling strength with Cu thickness—for example, by a perforation of the Cu layer—could be the cause of the sudden switching of the Ni magnetization to in plane. We therefore believe that it is indeed the angular dependence of the Ni anisotropy energy that leads to this behavior.

Qualitatively the canting of the Ni and Co magnetization directions resembles the suggested magnetic configuration of a 23 Å Co/10 Å Cu/53 Å Ni trilayer in a paper by Lauhoff *et al.*¹⁹ Quantitatively, however, the suggested tilt angles of 19° away from out of plane for Ni and 27° away from in plane for Co are not consistent with our data. Therefore, the alternative explanation of the authors, their results being determined by the domain structure of their samples, seems to be the more likely one.

V. CONCLUSION

The layer-resolved direct observation of the magnetic domain configuration in Co/Cu crossed wedges on Ni/Cu(001) revealed two different magnetic configurations as a function of Cu spacer layer thickness. The spin-reorientation transition in the Ni layer from out of plane to in plane for increasing coupling strength proceeds by a continuous canting of the Ni magnetization direction out of the perpendicular direction and a subsequent switching into an aligned phase, in which both magnetizations are in plane. In the canted phase the Ni canting angle can be tuned over a wide range of angles by adjusting the interlayer coupling strength via the Cu thickness. Such a canted magnetization might be technologically interesting to introduce a bias magnetization component perpendicular to the actual magnetization direction—for example, to influence the magnetic switching behavior in small elements. The presence of the two phases is attributed to the angle dependence of the magnetic anisotropy energy of Ni. From the phenomenological modeling a hysteretic behavior is expected in the switching between these two phases. To use such a behavior might be interesting for the design of magnetic elements that can be switched between more than only two magnetic states.

ACKNOWLEDGMENTS

We thank J. Gilles for help in the experiments and B. Zada and W. Mahler for technical assistance. Financial support by the German Minister for Education and Research (BMBF) under Grant No. 05 SL8EF19 is gratefully acknowledged.

- *Present address: Department of Physics and Astronomy, Louisiana State University, Baton Rouge, LA 70803-4001.
- ¹*Ultrathin Magnetic Structures*, edited by B. Heinrich and J. A. C. Bland (Springer, Berlin, 1994), Vol. 2.
 - ²M.D. Stiles, *J. Magn. Magn. Mater.* **200**, 322 (1999), and references therein.
 - ³P. Bruno and C. Chappert, *Phys. Rev. Lett.* **67**, 1602 (1991); P. Bruno, *Phys. Rev. B* **52**, 411 (1995).
 - ⁴J.E. Ortega, F.J. Himpsel, G.J. Mankey, and R.F. Willis, *Phys. Rev. B* **47**, 1540 (1993).
 - ⁵H.A.M. van den Berg, W. Clemens, G. Gieres, G. Rupp, M. Vieth, J. Wecker, and S. Zoll, *J. Magn. Magn. Mater.* **165**, 524 (1997).
 - ⁶C.H. Tsang, R.E. Fontana, Jr., T. Lin, D.E. Helm, B.A. Gurney, and M.L. Williams, *IBM J. Res. Dev.* **42**, 103 (1998).
 - ⁷G.A. Prinz, *J. Magn. Magn. Mater.* **200**, 57 (1999).
 - ⁸M. Rühlig, R. Schäfer, A. Hubert, R. Mosler, J.A. Wolf, S. Demokritov, and P. Grünberg, *Phys. Status Solidi A* **125**, 635 (1991).
 - ⁹A. Schreyer, J.F. Ankner, T. Zeidler, H. Zabel, M. Schäfer, J.A. Wolf, P. Grünberg, and C.F. Majkrzak, *Phys. Rev. B* **52**, 16 066 (1995), and references therein.
 - ¹⁰Shi-shen Yan, R. Schreiber, F. Voges, C. Osthöver, and P. Grünberg, *Phys. Rev. B* **59**, R11 641 (1999).
 - ¹¹J.C. Slonczewski, *Phys. Rev. Lett.* **67**, 3172 (1991).
 - ¹²J.C. Slonczewski, *J. Magn. Magn. Mater.* **150**, 13 (1995).
 - ¹³A. Taga, L. Nordström, P. James, B. Johansson, and O. Eriksson, *Nature (London)* **406**, 280 (2000).
 - ¹⁴P. Krams, F. Lauks, R.L. Stamps, B. Hillebrands, and G. Güntherodt, *Phys. Rev. Lett.* **69**, 3674 (1992).
 - ¹⁵M. Kowalewski, C.M. Schneider, and B. Heinrich, *Phys. Rev. B* **47**, 8748 (1993).
 - ¹⁶W.L. O'Brien and B.P. Tonner, *Phys. Rev. B* **49**, 15 370 (1994).
 - ¹⁷B. Schulz and K. Baberschke, *Phys. Rev. B* **50**, 13 467 (1994).
 - ¹⁸M. Farle, B. Mirwald-Schulz, A.N. Anisimov, W. Platow, and K. Baberschke, *Phys. Rev. B* **55**, 3708 (1997).
 - ¹⁹G. Lauhoff, A. Hirohita, J.A.C. Bland, J. Lee, S. Langridge, and J. Penfold, *J. Phys.: Condens. Matter* **11**, 6707 (1999).
 - ²⁰A. Scherz, F. Wilhelm, P. Pouloupoulos, H. Wende, and K. Baberschke, *J. Synchrotron Radiat.* **8**, 472 (2001).
 - ²¹J.L. Erskine and E.A. Stern, *Phys. Rev. B* **12**, 5016 (1975); G. Schütz, W. Wagner, W. Wilhelm, P. Kienle, R. Zeller, R. Frahm, and G. Materlik, *Phys. Rev. Lett.* **58**, 737 (1987).
 - ²²J. Stöhr, Y. Wu, M.G. Samant, B.B. Hermsmeier, G. Harp, S. Koranda, D. Dunham, and B.P. Tonner, *Science* **259**, 658 (1993).
 - ²³W. Kuch, R. Frömter, J. Gilles, D. Hartmann, Ch. Ziethen, C.M. Schneider, G. Schönhense, W. Swiech, and J. Kirschner, *Surf. Rev. Lett.* **5**, 1241 (1998).
 - ²⁴W. Kuch, J. Gilles, F. Offi, S.S. Kang, S. Imada, S. Suga, and J. Kirschner, *J. Electron Spectrosc. Relat. Phenom.* **109**, 249 (2000).
 - ²⁵H.P. Oepen, *J. Magn. Magn. Mater.* **93**, 116 (1991).
 - ²⁶A. Ney, F. Wilhelm, M. Farle, P. Pouloupoulos, P. Srivastava, and K. Baberschke, *Phys. Rev. B* **59**, R3938 (1999).
 - ²⁷J. Shen, J. Giergiel, and J. Kirschner, *Phys. Rev. B* **52**, 8454 (1995).
 - ²⁸J. Unguris, R.J. Celotta, and D.T. Pierce, *Phys. Rev. Lett.* **67**, 140 (1991).
 - ²⁹L. Néel, *C. R. Hebd. Seances Acad. Sci.* **255**, 1545 (1962); **255**, 1676 (1962).
 - ³⁰Y.T. Millev, H.P. Oepen, and J. Kirschner, *Phys. Rev. B* **57**, 5837 (1998); **57**, 5848 (1998).
 - ³¹H. Fritzsche, J. Kohlhepp, H.J. Elmers, and U. Gradmann, *Phys. Rev. B* **49**, 15 665 (1994).
 - ³²H.P. Oepen, M. Speckmann, Y. Millev, and J. Kirschner, *Phys. Rev. B* **55**, 2752 (1997).
 - ³³M. Farle, W. Platow, A.N. Anisimov, P. Pouloupoulos, and K. Baberschke, *Phys. Rev. B* **56**, 5100 (1997).
 - ³⁴C. Timm and P.J. Jensen, *Phys. Rev. B* **62**, 5634 (2000).
 - ³⁵E. P. Wohlfahrt, in *Ferromagnetic Materials*, edited by E.P. Wohlfahrt (North-Holland, Amsterdam, 1980), Vol. 1.
 - ³⁶B. Dieny and A. Vedyayev, *Europhys. Lett.* **25**, 723 (1994).
 - ³⁷A. Lessard, T.H. Moos, and W. Hübner, *Phys. Rev. B* **56**, 2594 (1997); X. Qian and W. Hübner, *ibid.* **64**, 092402 (2001).
 - ³⁸A. Moschel and K.D. Usadel, *Phys. Rev. B* **51**, 16 111 (1995).